Proc. Natl. Acad. Sci. USA
Vol. 82, pp. 8473–8477, December 1985
Biophysics

The 2-Å resolution structure of a thermostable ribonuclease A chemically cross-linked between lysine residues 7 and 41

(protein structure/thermostability/protein cross-linking/crystal lattice effects)

P. C. WEBER*, S. SHERIFF†, D. H. OHLENDORF*, B. C. FINZEL, AND F. R. SALEMME*

Protein Engineering Division, Genex Corporation, 16020 Industrial Drive, Gaithersburg, MD 20877

Communicated by J. Meinwald, August 19, 1985

ABSTRACT **The crystal structure of Lys-7-(dinitrophenylene)-Lys-41-cross-linked ribonuclease A has been determined by molecular replacement and refined by restrained least-squares methods to an R factor of 0.18 at 2.0-Å resolution. Diffraction intensity data were collected by using a conventional diffractometer and an x-ray area detector. Comparison of the thermostable cross-linked protein and the native enzyme shows them to be structurally similar, with a rms difference in backbone and side-chain atoms of 0.52 and 1.34 Å, respectively. Native and modified proteins additionally show 35 common bound solvent sites and similar overall temperature factor behavior, despite localized differences resulting from cross-link introduction, altered crystal pH, or lattice interactions with neighboring molecules. These results are discussed in the context of proposals on the origins of thermostability in the cross-linked enzyme.**

Bovine pancreatic RNase A is a small 124-residue protein catalyzing the cleavage of single-stranded RNA. RNase A was among the first enzymes to be structurally characterized by x-ray crystallography (1) and has been the subject of numerous investigations of protein stability and folding. Here we report the crystal structure determination of RNase A that has been chemically cross-linked by reaction with 1,5-difluoro-2,4-dinitrobenzene to produce an adduct with dinitrophenylene (DNP) covalently linking the ε-amino groups of RNase lysine residues 7 and 41. The structure determination was motivated by recent reports on the thermal unfolding properties of Lys-7-(DNP)-Lys-41-cross-linked RNase (2). These studies showed that at pH 2, the cross-linked protein melted at a temperature some 25°C higher than the native enzyme under similar conditions. Introduction of the DNP cross-link catalytically inactivates RNase A and thus eliminates enzyme assays as a test of protein structural integrity. Consequently, the structure determination of the modified protein was carried out to establish the nature and extent of structural alterations resulting from cross-link formation.

METHODS

Crystals and Data Collection. DNP-cross-linked RNase was crystallized from 30% (vol/vol) ethanol/water solutions buffered at pH 8.0 (3). Crystals belong to the orthorhombic space group $P2_12_12_1$, with $a = 37.05$ Å, $b = 41.26$ Å, and $c = 75.64$ Å and contain a single molecule per crystallographic asymmetric unit. Two sets of x-ray diffraction intensities, collected by different methods, were used in the structure determination.

A diffractometer data set was collected on a Kriselcontrolled Huber diffractometer utilizing an Elliott GX-21 x-ray source. The data set included measurements of all unique reflections from infinity to 2.0-Å resolution, together with Friedel mates in a shell from 2.1- to 2.0-Å resolution. Intensity data were collected as step scans and subsequently integrated (4), corrected for background, absorption (5), Lorentz polarization, and radiation damage effects (6). A total of 10,701 observations of 8301 unique reflections was collected. The scaling R factor on intensity (I) for 3443 symmetry-related reflections (Friedel mates in the 2.1- to 2.0-Å resolution range and zonal reflections throughout reciprocal space) was 0.081.

Another set of diffraction intensities was collected by using a Xentronics area detector mounted on a modified Supper oscillation camera, also utilizing the GX-21 rotating anode x-ray source. The detector was mounted 12 cm from the crystal with an angle of 20° between the detector normal and the x-ray beam. In this configuration, data from infinity to 2.2-Å resolution were intercepted by the Xentronics detector face. Data were collected as a succession of oscillation frames, each corresponding to a 512 × 512 × 8 bit digitized image of the diffraction pattern integrated over a 10-min oscillation range. Individual frames were written to magnetic tape and subsequently processed as described by Durbin *et al.* (7). A total oscillation range of 183° was scanned during 22 hr of x-ray exposure to collect 13,282 observations of 5213 unique reflections. The Xentronics data scaled with an internal R factor of 0.038 (on I) and scaled to the diffractometer data with an overall R factor of 0.065. In the combined data set, 99% of the theoretically possible reflections to 2-Å resolution were measured with 95% having $I > \sigma(I)$.

Structure Determination. The structure of cross-linked RNase (RNase X) was solved by molecular replacement using Patterson search methods. Refined coordinates for RNase A (8) were obtained from the Brookhaven Protein Data Bank (9) and used for the generation of probe Patterson maps. The initial solution proceeded in three stages.

The first stage applied the rotation function to determine the angular orientation of the RNase A probe molecule in the RNase X crystal cell. RNase A coordinates were positioned in an orthogonal P1 cell with 90-Å edges and transformed to produce coefficients for a probe Patterson incorporating structure factors from 4- to 10-Å resolution. The 4500 highest peaks abstracted from the probe Patterson in a 5- to 20-Å shell about the origin, together with a corresponding peak set computed from the RNase X intensity data, were used as input to the Patterson rotation function (10, 11) incorporated in the PROTEIN crystallographic software system (12).

The publication costs of this article were defrayed in part by page charge payment. This article must therefore be hereby marked "*advertisement*" in accordance with 18 U.S.C. §1734 solely to indicate this fact.

Abbreviations: DNP, dinitrophenylene; RNase X, cross-linked RNase.

*Present address: Central Research & Development Department, E. I. du Pont de Nemours and Co., Experimental Station, Building 328, Room B25, Wilmington, DE 19898.

†Present address: Laboratory of Molecular Biology, National Institute of Arthritis, Diabetes, Digestive and Kidney Diseases, Bethesda, MD 20205.

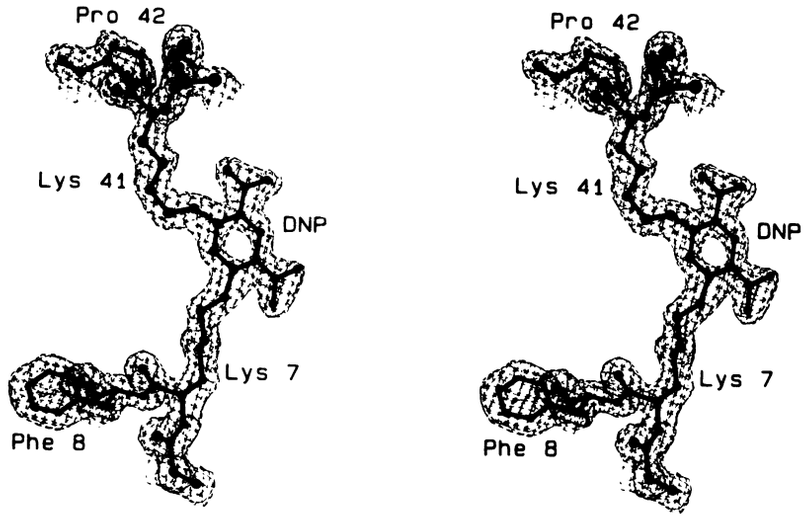

FIG. 1. Stereoscopic view showing the final $2F_o - F_c$ electron density map and refined model for the DNP cross-linking group and adjacent amino acid residues.

Initial searches on 5° increments over a range appropriate to the RNase X cell Patterson symmetry (13) revealed a major correlation peak 6.6 σ above background. The angular orientation was then refined by a 1° grid search in the vicinity of the peak.

The second stage applied the translation function (14) to establish the position of the rotationally oriented probe molecule in the RNase X crystal cell. Separate searches were made in orthogonal Patterson cell planes to locate superposition peaks relating molecules by the $P2_12_12_1$ crystallographic screw axes. Major peaks found in each plane produced a consistent solution defining the probe molecule translational position. Combination of the rotation and translation results produced an initial orientation that gave a crystallographic R factor of 0.44 computed on data from 15- to 6-Å resolution.

The probe molecule orientation was refined as a rigid body by using the program CORELS (15), which altered the initial orientation angles and displacements by about 5° and 1 Å, respectively. The crystallographic R factor computed from the refined probe orientation was 0.33 based on data from 15- to 6-Å resolution and 0.38 on 20- to 3-Å data. These results, together with difference Fourier syntheses that clearly showed the DNP group, provided evidence of the correctness of the molecular replacement solution.

Structure Refinement. The oriented RNase A coordinates were transformed and combined with the observed RNase X structure factor amplitudes to produce an initial electron density map using coefficients [$2F_o$(RNase X) − F_c(RNase A)] and the model phases. The structure was then rebuilt into the modified electron density map using an Evans and Sutherland PS300 graphics system. Atomic positions and thermal parameters of the adjusted model were refined in 40 cycles by using the restrained least-squares method of Hendrickson and Konnert (16), modified to incorporate fast Fourier transform algorithms of Ten Eyck (17) and Agarwal (18). Initial refinement cycles incorporated data from 20- to 3-Å resolution, followed by gradual extension to include data to 2.0-Å resolution. Coordinates for the cross-link were included in the refinement model when examination of a 2.2-Å difference Fourier map clearly revealed the orientation of the DNP group. The final RNase X model incorporates 75 bound solvent molecules and has a crystallographic R factor of 0.184 for all 7853 reflections with $I > \sigma(I)$ to 2.0-Å resolution. Fig. 1 shows representative electron density in the final map in the vicinity of the DNP cross-link. Refined model characteristics for RNase X and RNase A are summarized in Table 1.

RESULTS

Structural Comparison of RNase A and RNase X. Fig. 2 *Upper* shows a superposition of the RNase A (8) and RNase X backbone structures (based on least-squares fit of all atoms common to both molecules) together with the location of the chemically introduced DNP cross-link.

The cross-link connects Lys-7 on the RNase X amino terminus α-helix with Lys-41 at the edge of the extended antiparallel β-sheet comprising most of the remainder of the molecule. Comparisons have been made here with the native structure determined by Wlodawer and Sjolin (8), owing to the similar data resolution and refinement methods used in the structure determinations. The structures are very similar overall, with a rms difference in backbone atom positions of 0.52 Å and in side chain positions of 1.34 Å (Fig. 3). With the exception of the cross-linked lysine side chains and some

Table 1. Comparison of least-squares refinement parameters for RNase A and RNase X

Parameter	RNase A	RNase X
Resolution limits	10.0–2.0 Å	20.0–2.0 Å
Reflections	7708	7853
	$I > 3\sigma(I)$	$I > \sigma(I)$
Crystallographic R factor	0.159	0.184
Protein atoms	951	951
Water molecules	128	75
Geometric conformity*		
Distances		
1—2	0.025 Å	0.024 Å
1—3	0.065 Å	0.038 Å
1—4	0.067 Å	0.044 Å
Planes		
Peptides	0.022 Å	0.022 Å
Other	0.007 Å	0.009 Å
Chiral volumes	0.215 Å^3	0.283 Å^3
Thermal parameters		
1—2	0.967 Å^2	1.056 Å^2
1—3	1.580 Å^2	1.634 Å^2

RNase A parameters are from ref. 8 or are computed from data deposited in the Brookhaven Protein Data Bank (9).

*Values given are the rms deviation from ideal geometry. Thermal parameter values are the mean difference in isotropic temperature factor between pairs of atoms. The notation 1—2, 1—3, and 1—4 refers to atoms pairs related through a bond, a bond angle, or torsion angle, respectively.

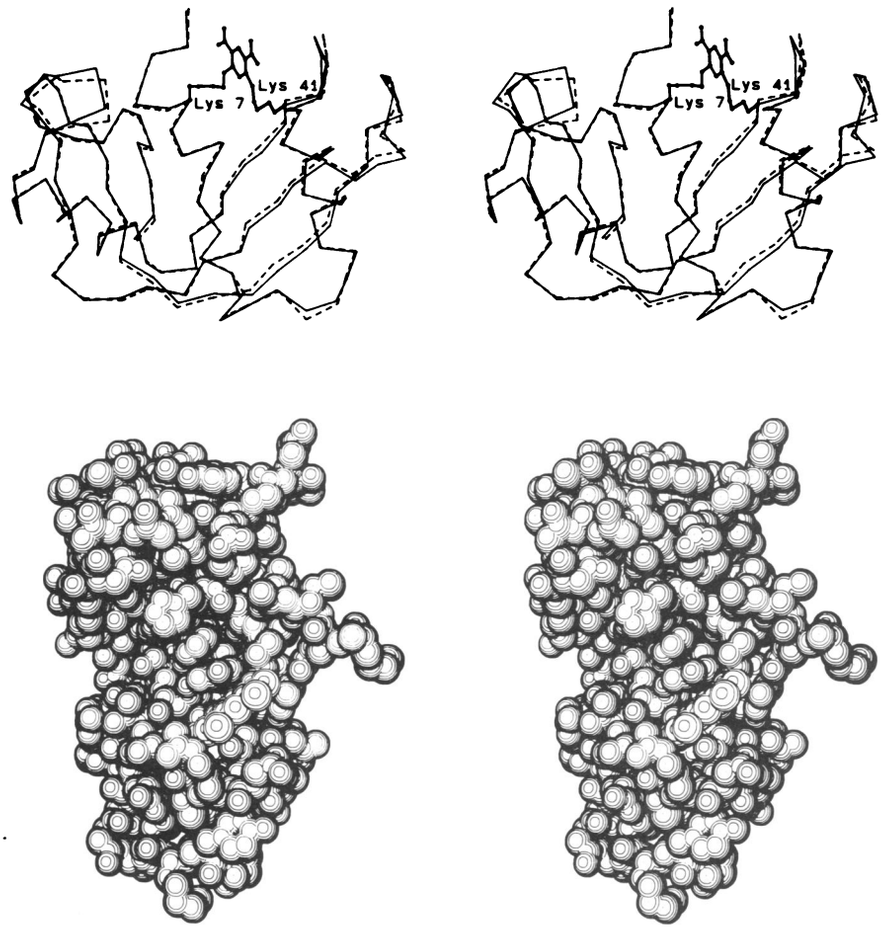

FIG. 2. (*Upper*) Stereoscopic views of DNP-cross-linked RNase (solid lines) superimposed on RNase A. (*Lower*) A space filling representation of the cross-linked protein that illustrates the packing about the DNP group (lightly contoured and slightly below and to the right of center).

adjacent residues (Fig. 4), differences in conformation generally reflect alternative lattice contacts made in the RNase A and RNase X crystal cells. A comparison of the 75 refined solvent molecules found in RNase X with the 128 localized in RNase A shows that 35 positions are common (rms error < 1 Å) to both molecules.

Alterations Associated with Cross-Link Introduction. Fig. 4 shows a comparison of the local structural environments of lysine residues 7 and 41 in the native and cross-linked proteins. The observed alterations reflect steric effects of cross-link group introduction, together with differences due to crystal pH and phosphate ion concentration. In the RNase A structure determined with phosphate present at pH 5.3, the side chain of Lys-7 is solvent exposed at the molecular surface, and Lys-41 forms an ionic or hydrogen bond with an oxygen of inorganic phosphate bound to the imidazole group of His-12 at the enzyme active site. In RNase X, the side chains of lysine residues 7 and 41 reorient to allow formation of the DNP cross-link. Steric interactions formed with the lysine side chains or the DNP group cause small shifts (0.5–1 Å rms) in adjacent side chains of Gln-11 and Arg-39. In addition, a change also occurs in the side chain orientation of His-119, which together with His-12 and Lys-41, plays a central role in the RNase catalytic mechanism. The reorientation of His-119 may reflect differences in the crystal pH between RNase A (pH 5.3) and RNase X (pH 8.0) and absence of bound phosphate in RNase X. The higher pH of the RNase X crystals may result in deprotonation of the His-119 imidazole group and the accompanying loss of the hydrogen bond formed between His-119 and Asp-121 in the native structure. Concomitantly, lack of a bound phosphate ion in RNase X could result in loss of interactions stabilizing the active site arrangement in RNase A or simply provide space allowing His-119 reorientation. We find no evidence in the RNase X electron density map for an alternative His-119 conformation similar to that reported by Moss *et al.* (19) in RNase A.

Comparative Temperature Factor Behavior. Atomic temperature factors (B values) obtained during crystallographic refinement give estimates of protein dynamical behavior in solution (20). Fig. 3 compares the backbone B-value behavior in RNase A and RNase X and shows that B-value variations are slightly larger in the cross-linked protein. This could result from increased local flexibility of the cross-linked enzyme, differences in lattice packing interactions (21), or the occurrence of lattice disordering phenomena whose effects are manifest in refined B-value behavior (22). Despite these differences, comparison of the molecules yields a correlation coefficient of 0.60 that is typical of many protein structures determined in alternate crystal forms (21). Moreover, the average B value for atoms of the DNP cross-link is 23 $Å^2$, a value comparable to other exposed side chains or the more flexible regions of the protein backbone. These results suggest that the introduction of the DNP cross-link has no major effect on the folded proteins dynamical behavior and, most notably, does not decrease RNase flexibility in the crystal lattice.

DISCUSSION

The preceding shows that the basic structural organization of RNase A is unaltered by the introduction of a DNP cross-link

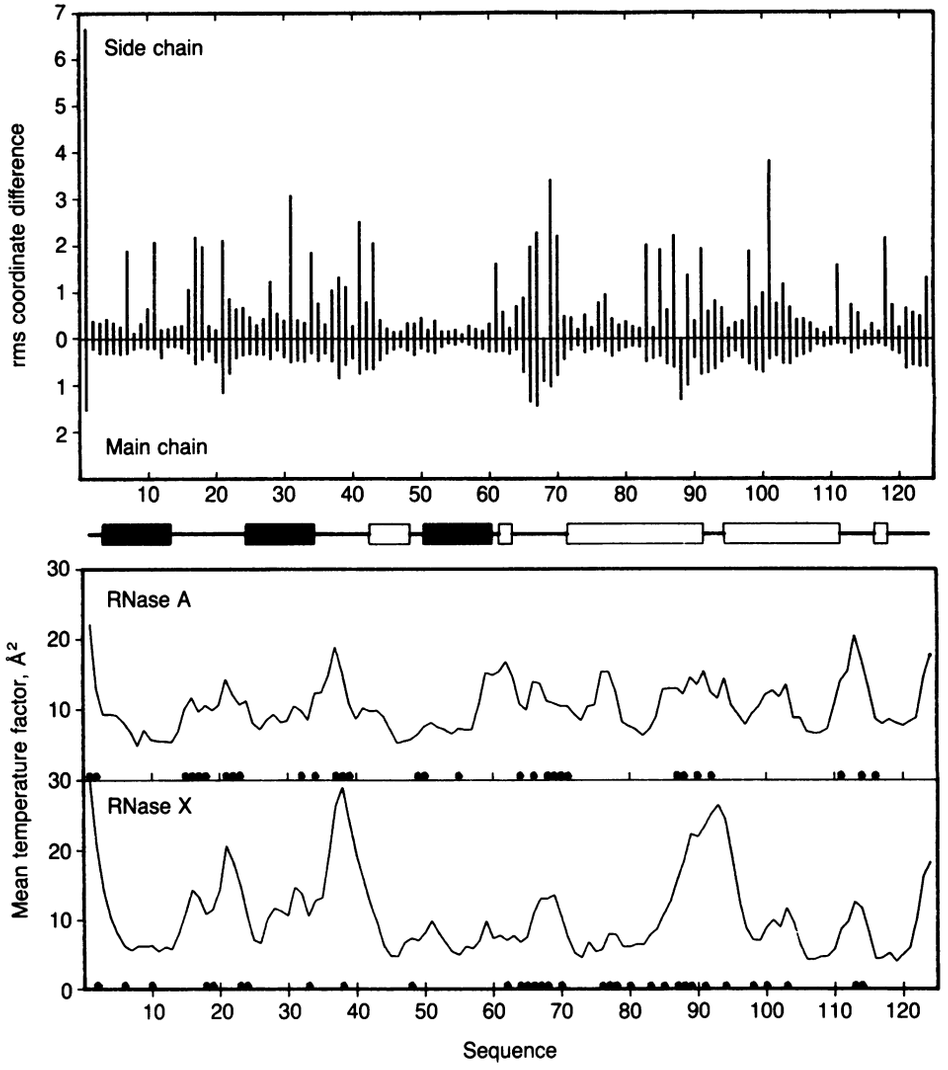

FIG. 3. Comparison of the refined structures of RNase A and RNase X. (*Top*) rms positional differences averaged over backbone and side chain residues after least-squares superposition of the structures. (*Middle*) Molecular secondary structure with α-helices as black bars, β-sheet strands as open bars, and connecting loops as lines. (*Bottom*) Average backbone B-value behavior for the molecules as connected curves together with positions of surface residues involved in crystal contacts (dots).

between lysine residues 7 and 41. Differences that do occur between RNase A and RNase X are attributable to three sources. These include local conformational changes resulting from steric interactions near the cross-link, differences in crystal pH and phosphate content that cause a reorientation of His-119, and numerous changes in surface residues or loops that reflect alternative lattice contacts in the different crystal cells. Additional similarities in the structures include the common situation of 35 bound solvent molecules and similar B-value behavior. Although crystal interactions are known to influence side chain conformation, solvent binding, and B-value behavior (21, 22), observed differences between RNase A and RNase X are all typical of structures of the same protein determined in different crystal environ-

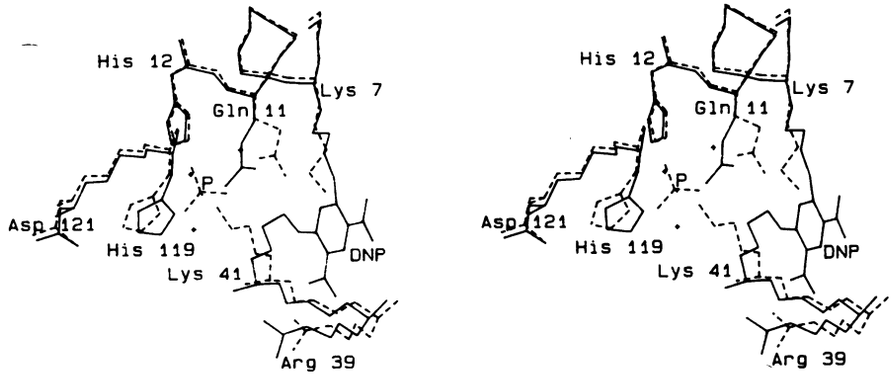

FIG. 4. Stereoscopic view comparing the local environments of Lys-7 and Lys-41 in RNase X (solid lines) and RNase A (dashed lines). Note that RNase A has a phosphate ion (P) bound to His-12, one of whose oxygen atoms is replaced by a bound water molecule (small cross) in RNase X.

ments (21, 23) and reminiscent of differences observed previously between RNase S and an isomorphous derivative with DNP covalently linked to Lys-41 (24).

Recent studies comparing the thermal unfolding properties of RNase A and RNase X at pH 2 have shown that the cross-linked protein melts some 25°C higher than the native enzyme (2). This difference in behavior was attributed to entropic effects that altered the relative free energies of folding the native and cross-linked proteins. Specifically, the stabilization of RNase X was ascribed to a reduction in conformational entropy that predominantly manifests itself in the proteins unfolded state. This results in a destabilization of the unfolded state of the cross-linked molecule relative to the folded states of RNase X and RNase A (2). Implicit in this comparison of RNase A and RNase X is the assumption that the folded molecules' free energies are essentially equivalent. The present results suggest that, apart from local changes due to chemical modification, bonded interactions contributing enthalpic components of the free energy are essentially conserved in the two structures. Moreover, to the extent that the B-value behavior is indicative of the folded proteins' dynamic behavior, the observed similarities suggest that conformational entropic components of the folded molecules' free energy are also similar. Differences that do occur generally typify lattice packing effects that effectively trap one of numerous conformational states simultaneously present in solution (22, 23). Although charged group interactions might also influence the relative stabilities of RNase A and RNase X, the present results are consistent with the proposal (2) that the differences in stability between the native and cross-linked proteins primarily reflect entropic effects manifest in the molecules' unfolded states. It is notable in this context that comparisons of native and thermolabile mutants of T4 phage lysozyme (25) have previously shown the essential preservation of the native structure in crystals. This may suggest that differences in thermal stability between native and mutant proteins also reflect effects manifest in the molecules' unfolded states, although these presumably differ from the conformational entropy effects resulting from cross-link introduction into RNase A.

Coordinates for RNase X have been deposited in the Brookhaven Protein Data Bank (9).

We thank Dr. A. Wlodawer of the National Bureau of Standards for RNase A structural data and useful discussions.

1. Kartha, G., Bello, J. & Harker, D. (1967) *Nature (London)* **213,** 862–865.
2. Lin, S. H., Konishi, Y., Denton, M. E. & Scheraga, H. A. (1984) *Biochemistry* **23,** 5504–5512.
3. Weber, P. C., Salemme, F. R., Lin, S. H., Konishi, Y. & Scheraga, H. A. (1985) *J. Mol. Biol.* **181,** 453.
4. Hanson, J. C., Watenpaugh, K. D., Sieker, L. & Jensen, L. H. (1979) *Acta Crystallogr.* **A35,** 616–621.
5. North, A. C. T., Phillips, D. C. & Mathews, F. S. (1968) *Acta Crystallogr.* **A24,** 351.
6. Hendrickson, W. A. (1976) *J. Mol. Biol.* **106,** 889–893.
7. Durbin, R. M., Burns, R., Moulai, J., Metcalf, P., Freymann, D., Blum, M., Anderson, J. A., Harrison, S. C. & Wiley, D. C. (1985) *Science*, in press.
8. Wlodawer, A. & Sjolin, L. (1983) *Biochemistry* **22,** 2720–2728.
9. Bernstein, F. C., Koetzle, T. F., Williams, G. J. B., Meyer, E. F., Jr., Brice, M. D., Rodgers, J. R., Kennard, O., Shimanouchi, T. & Tasumi, M. (1977) *J. Mol. Biol.* **112,** 535–542.
10. Huber, R. (1965) *Acta Crystallogr.* **A19,** 353–356.
11. Fehlhammer, H. & Bode, W. (1975) *J. Mol. Biol.* **98,** 683–692.
12. Steigemann, W. (1974) Dissertation (Technische Universitat Munchen, Munich, Federal Republic of Germany).
13. Rao, S. N., Ji, J.-H. & Hartsuck, J. A. (1980) *Acta Crystallogr.* **A36,** 878–884.
14. Crowther, R. A. & Blow, D. M. (1967) *Acta Crystallogr.* **23,** 544–548.
15. Sussman, J. L., Holbrook, S. R., Church, G. M. & Kim, S.-H. (1977) *Acta Crystallogr.* **A33,** 800–804.
16. Hendrickson, W. A. & Konnert, J. H. (1980) in *Computing in Crystallography*, eds. Diamond, R., Ramseshan, S. & Venkatesan, K. (Indian Institute of Science, Bangalore, India), pp. 13.01–13.23.
17. Ten Eyck, L. F. (1973) *Acta Crystallogr.* **A29,** 183–191.
18. Agarwal, R. C. (1978) *Acta Crystallogr.* **A34,** 791–809.
19. Moss, D. S., Haneff, I. & Howlin, B. (1984) *Trans. Am. Crystallogr. Assoc.* **20,** 123–127.
20. Karplus, M. & McCammon, J. A. (1983) *Annu. Rev. Biochem.* **53,** 263–300.
21. Sheriff, S., Hendrickson, W. A., Stenkamp, R. E., Sieker, L. C. & Jensen, L. H. (1985) *Proc. Natl. Acad. Sci. USA* **82,** 1104–1107.
22. Finzel, B. C. & Salemme, F. R. (1985) *Nature (London)* **315,** 686–688.
23. Marquart, M., Walter, J., Deisenhofer, J., Bode, W. & Huber, R. (1983) *Acta Crystallogr.* **B39,** 480–490.
24. Allewell, N. M., Mitsui, Y. & Wyckoff, H. N. (1973) *J. Biol. Chem.* **248,** 5291–5298.
25. Grutter, M. G., Hawkes, R. B. & Matthews, B. W. (1979) *Nature (London)* **277,** 667–669.